

Numerical simulations of light bullets using the full-vector time-dependent nonlinear Maxwell equations

Peter M. Goorjian

NASA Ames Research Center, Moffett Field, California 94035-1000

Yaron Silberberg

The Weizmann Institute of Science, 76100 Rehovot, Israel

Received December 16, 1996; revised manuscript received March 13, 1997

The vector Maxwell's equations are solved to simulate propagating and colliding optical pulses in planar waveguides. The slowly varying envelope approximation is not made, and therefore the dynamics of the optical carrier are retained in the calculations. Some short optical pulses are found to be essentially unchanged over rather long propagation distances and stable over some energy variation in a manner characteristic of light bullets. With greater energy increase the pulses do not collapse, as predicted by the nonlinear Schrödinger equation; rather, after initially compressing, they undergo unlimited expansion. Because the optical pulses that are employed in these simulations are extremely short, they are beyond the limitations of the slowly varying envelope approximation that is used in the derivation of the nonlinear Schrödinger equation. The dispersive effects are modeled by a single Lorentzian resonance, and the nonlinear refraction is modeled by a Kerr-like instantaneous nonlinearity. The procedure for obtaining numerical solutions to the nonlinear Maxwell equations is described, and solutions are obtained by a finite-difference algorithm. © 1997 Optical Society of America [S0740-3224(97)02411-9]

1. INTRODUCTION

Using the exact Maxwell's equations, researchers have obtained¹ solutions that have characteristics that are similar to light bullets,² i.e., stable optical pulses that are self-supporting under the effects of diffraction, anomalous dispersion, and nonlinear refraction. The pulse propagation is in a planar waveguide, where diffraction is limited to one transverse direction. Some of these pulses propagate without any essential changes in shape or spectral content over relatively large distances in comparison with their Rayleigh ranges and are stable to some energy variation. Furthermore, when the energy in these pulses is increased further, after initially contracting, they undergo unlimited expansion. By contrast, standard theory, which uses the nonlinear Schrödinger equation (NLSE) (an approximation to Maxwell's equations), predicts² that by increasing the energy of a pulse beyond a critical value, self-focusing will lead to the collapse of optical pulses. Also, additional calculations with Maxwell's equations show that, when two of these pulses are counterpropagating and are displaced slightly from a head-on approach, upon colliding, they change each other's trajectories, although they retain their self-support, in the manner of solitons. These pulses are extremely short, varying from approximately 9 to 18 fs in duration (for the full width at half-maximum intensity of the pulse), and they vary from roughly 1.25 to 2.5 μm long and contain roughly 3 to 5 optical cycles.

The solutions are computed by solving the time-dependent vector nonlinear Maxwell's equations in two space dimensions.³⁻⁶ The linear dispersion is modeled

by a Lorentzian model⁷ with a single resonance, and the nonlinear refraction is modeled by a Kerr-like⁷ instantaneous nonlinearity. The optical carrier is retained in the calculations so that each wavelength in the pulse is resolved. Also, since the Maxwell's equations are solved exactly, all higher-order effects,^{8,9} such as higher-order dispersion, shock formation, self-frequency shift, space-time focusing, and modulations of the optical carrier, are automatically accounted for in these simulations.

For comparison, standard methods of analysis and numerical simulation use the NLSE and its generalizations.^{7,8} The NLSE solves for the propagation of the envelope of the pulse, and it assumes that the envelope is slowly varying.^{7,8} Also, terms must be added to the NLSE to account for higher-order effects.^{8,9} The NLSE cannot be used for the simulations of the short pulses in this study, but it may be possible to use a generalization of the NLSE with sufficient additional terms to properly account for these propagating and colliding short pulses.

There has been an extensive amount of research in the past 25 years in the areas of short-pulse dynamics, both theoretical and experimental: self-focusing effects, light bullets, and the limitations of the standard NLSE. Research in these areas is represented by the following sample of papers.

In the area of the generation and modeling of ultrashort pulses, Fork *et al.*¹⁰ generated 6-fs pulses by using extracavity pulse compression. Using intracavity pulse compression, Asaki *et al.*¹¹ generated 11-fs pulses and Zhou *et al.*¹² generated sub-10-fs pulses. High-

energy ultrashort pulses in fibers were generated by Walton *et al.*¹³ The shortest pulses obtained so far were produced by Baltuska *et al.*¹⁴; they used pulse compression to obtain 5-fs pulses at a 1-MHz repetition rate. Christov *et al.*^{15–17} simulated short-pulse propagation in a Ti:sapphire laser crystal, including the effects of higher-order dispersion and space–time focusing. In the area of self-focusing,^{18–21} Huang *et al.*¹⁸ simulated self-focusing for use in laser mode locking. Luther *et al.*^{19,20} studied self-focusing thresholds and collapse in normally dispersive media. Kewitsch and Yariv²¹ looked at self-focusing and self-trapping of optical beams upon photopolymerization, both theoretically and experimentally. There has been experimental work in the area of high-power short pulses for self-focusing by Liu and Umstadter,²² by Braum *et al.*,²³ and by Brodeur *et al.*²⁴ Here the self-focusing effects interact with the defocusing effects of the plasma that were created by the intense laser pulse. A self-channeling model was proposed by Braum *et al.*,²³ whereas Brodeur *et al.*²⁴ advocated a moving-focus²⁵ alternative. An attempt to generate light bullets in fused silica was made by Sucha.²⁶ Simulations of light bullets were made by Chen and Atai²⁷ for dark optical bullet beams and by Snyder and Mitchell²⁸ for bullet beams in a saturable medium. Several papers^{29–33} have examined the limitations of the NLSE. Rothenburg^{29,30} looked at the breakdown of the NLSE during self-focusing of femtosecond pulses. Akhmediev and Ankiewicz³¹ examined the limits of the NLSE for beam propagation. Snyder *et al.*³² showed that birefringence requires the use of Maxwell's equations. And Hayata and Koshiba³³ looked at the effects of cross-phase modulations on the propagation of multidimensional solitons.

The numerical algorithm employed in this paper is described in Refs. 3–6. It was used for calculations of propagating and interacting temporal^{3,4,6} and spatial^{5,6} solitons. In those simulations the nonlinear effects included Kerr-like instantaneous as well as Raman dispersive nonlinearities. Convolution integrals described the linear and nonlinear dispersive effects. The polarization was determined by a coupled system of nonlinear, ordinary differential equations. Those equations were nonlinearly coupled to Maxwell's equations through the electromagnetic field. That entire system of equations was solved by a finite-difference algorithm, as described in Ref. 4. With that algorithm development it became possible, for the first time, to solve the nonlinear, vector Maxwell's equations exactly, without having to use approximations such as the NLSE or its generalizations. In this paper the algorithm from Ref. 4 is used under the simplification that the nonlinearity is entirely instantaneous, i.e., all Kerr-like.

To isolate each material effect on the optical wave, a methodical sequence of calculations was performed. In the first calculation, only dispersion acted on a pulsed plane wave. Next diffractive effects on a beam were calculated. These two linear effects were then allowed to act together on a pulse so that parameters could be determined for which the spreading rates of the pulse owing to dispersion and diffraction were approximately equal. Next, nonlinear refraction was introduced as the third effect, and a pulse power was found so that a self-

supporting pulse resulted. Finally, two of these pulses were propagated toward each other, slightly off center in approach, and, while colliding, they attracted each other. Additional calculations were performed to determine the effects on the pulse when its energy was varied.

The calculations presented in this paper use a nonlinear material for which the dispersive parameters are fictitious. The purpose of these calculations was to investigate the properties of very short pulses (approximately 10–20 fs), as determined by the vector Maxwell equations. However, it may be possible to obtain similar computational results with realistic material parameters. For example, there are highly nonlinear glasses³⁴ with nonlinear indices of refraction that are approximately 40 times stronger than that of the silica glass that is modeled in this paper. Hence the power requirements for the optical pulse would be lowered equivalently. Also, these glasses have strongly dispersive properties with strong negative group-velocity dispersion (GVD) at wavelengths further into the infrared region than that used here.

The use of Maxwell's equations without making the slowly varying envelope approximation is being applied to other problems in nonlinear optics. In Ref. 35 the question of shock waves on the optical carrier is studied, and in Ref. 36 the dynamic nonlinear optical skin effect is modeled. Also, in Ref. 37, short-pulse propagation in semiconductor materials under the effects of quantum interactions with the electrons is investigated by solving the Maxwell–Bloch equations without making either the slowly varying envelope or rotating-wave approximations.

2. GOVERNING EQUATIONS

The full-vector time-dependent nonlinear Maxwell equations are solved without making the standard slowly varying envelope approximation (the approximation that is made in the NLSE). Also, the optical carrier is retained in the optical pulse, and it is accurately resolved in the calculations. In addition, the linear dispersion, which is described by a convolution integral, is evolved by solving an ordinary differential equation. The finite-difference algorithms that are used to solve the differential equations are described in Ref. 4. In fact, these algorithms are also capable of including nonlinear dispersive effects, such as Raman scattering. In this paper the nonlinearity is entirely instantaneous, i.e., all Kerr-like.

A. Maxwell's Equations and the Polarization Equation

Consider a two-dimensional problem, with fields that are bound in the y direction, such as in a planar waveguide that limits pulse propagation to movement in the x – z plane. We assume a transverse-magnetic wave, with the y component, E_y , of the electric field and the x and z components, H_x and H_z , respectively, of the magnetic field, varying in the x – z plane.

Then Maxwell's equations are given by

$$\frac{\partial D_y}{\partial t} = \frac{\partial H_x}{\partial z} - \frac{\partial H_z}{\partial x}, \quad \frac{\partial \mu_0 H_x}{\partial t} = \frac{\partial E_y}{\partial z}, \quad \frac{\partial \mu_0 H_z}{\partial t} = -\frac{\partial E_y}{\partial x}, \quad (1)$$

and the polarization equation for D_y is given by

$$D_y = \epsilon_0 \epsilon E_y = \epsilon_0 \epsilon_\infty E_y + P_y, \quad P_y = P_y^L + P_y^{\text{NL}}. \quad (2)$$

Here μ_0 and ϵ_0 are the permeability and permittivity coefficients for free space, ϵ is the relative material permittivity, ϵ_∞ is the relative material permittivity at infinite frequency, D_y is the y component of the electric displacement, and P_y is the y component of the electric polarization. The polarization, P_y , is assumed to consist of two parts^{4,8}: a linear part, P_y^L , and a nonlinear part, P_y^{NL} .

The linear polarization, P_y^L , is given by a convolution of $E_y(x, z, t)$ and the first-order susceptibility function, $\chi^{(1)}(t)$. Assuming that the electromagnetic field and the susceptibility function are equal to zero for $t \leq 0$, the linear polarization is given by

$$P_y^L(x, z, t) = \epsilon_0 \int_0^t \chi^{(1)}(t - \bar{t}) E_y(x, z, \bar{t}) d\bar{t}. \quad (3)$$

The susceptibility function, $\chi^{(1)}(t)$, describes a material having a Lorentz linear dispersion and is given^{7,38} by the following function:

$$\chi^{(1)}(t) = \left(\frac{\omega_p^2}{\nu_0} \right) \exp(-\delta t/2) \sin(\nu_0 t). \quad (4)$$

The corresponding linear permittivity as a function of frequency is given by

$$\epsilon(\omega) = \epsilon_\infty + \chi^{(1)}(\omega) = \epsilon_\infty + \frac{\omega_0^2(\epsilon_s - \epsilon_\infty)}{\omega_0^2 - j\delta\omega - \omega^2}, \quad (5)$$

where $\omega_p^2 = \omega_0^2(\epsilon_s - \epsilon_\infty)$ and $\nu_0^2 = \omega_0^2 - \delta^2/4$. Here ω_0 is the resonance frequency, ω_p is the plasma frequency, ϵ_s is the relative static material permittivity, and δ is the damping rate.

The equation that is used for the nonlinear polarization, P_y^{NL} , is obtained by making the following approximation. Let a material be described by a nondispersive, nonlinear material permittivity; then⁸

$$\begin{aligned} \epsilon &= n_T^2 = (n + n_2 |E_y|^2)^2 \\ &= n^2 \left(1 + \frac{n_2}{n} |E_y|^2 \right)^2 \\ &\approx \epsilon_\infty \left(1 + \frac{2n_2}{n} |E_y|^2 \right) \\ &= \epsilon_\infty (1 + \epsilon_0 c n_2^I |E_y|^2) \\ &= \epsilon_\infty \left(1 + \frac{n_2^I}{\eta_0} |E_y|^2 \right), \end{aligned} \quad (6)$$

where c is the speed of light in free space; η_0 is the impedance of free space; n_T is the index of refraction; n is the linear index of refraction, $\epsilon_\infty = n^2$; n_2 is the nonlinear index of refraction, measured in (meters/volt)²; n_2^I is the nonlinear index of refraction, measured in (meters²/watt); and⁸ $n_2^I = 2n_2/(\epsilon_0 c n)$.

With this approximation the nonlinear polarization, P_y^{NL} , is given by

$$P_y^{\text{NL}} = \epsilon_0 \epsilon_\infty \frac{n_2^I}{\eta_0} |E_y|^2. \quad (7)$$

B. Solution Procedure

The evolution of the electromagnetic field, given by E_x , H_x , and H_z , is found by solving Eqs. (1) and (2), with P_y determined by Eqs. (3) and (7). A new procedure for solving these equations was introduced in Ref. 3. In that reference the linear dispersion, P_y^L , which is described by the convolution integral in Eq. (3), is evolved by solving an ordinary differential equation. Then the polarization equation, Eq. (2), is used to determine E_y at the new time, with D_y at the new time found by solving Maxwell's equations.

The differential equation for P_y^L is obtained as follows. The kernel $\chi^{(1)}(t)$ in Eq. (3), as given in Eq. (4), satisfies the homogeneous linear differential equation

$$\frac{d^2 \chi^{(1)}(t)}{dt^2} + \delta \frac{d\chi^{(1)}(t)}{dt} + \omega_0^2 \chi^{(1)}(t) = 0. \quad (8)$$

By differentiating P_y^L , as given in Eq. (3), and using Eq. (8), we find P_y^L to satisfy³

$$\frac{d^2 P_y^L(t)}{dt^2} + \delta \frac{dP_y^L(t)}{dt} + \omega_0^2 P_y^L(t) = \epsilon_0 \omega_p^2 E_y(t). \quad (9)$$

For considerations in developing the numerical algorithm, Eq. (9) is modified by use of Eq. (2) for D_y . The complete details of the solution procedure and the finite-difference equations are given in Ref. 4.

C. Pulse Description

An optical pulse is introduced into the computational domain as a time-varying boundary condition at the middle of the left-hand boundary. Initially, the electromagnetic field inside the domain is set to zero. The pulse is given by specifying the electric field at the entrance to the material at $z = 0$ by

$$E_y(x, 0, t) = E_0 \operatorname{sech}[(t - T_D)/T_0] \sin(\omega_c t) \operatorname{sech}(x/X_0). \quad (10)$$

Note that the factor $\sin(\omega_c t)$ that describes the optical carrier is retained in the description of the pulse.

3. COMPUTATIONAL RESULTS: LIGHT BULLETS

We show the results by displaying the variation of the electric field in the computational domain. The computational domain is 62 μm along the direction of propagation and 21 μm in the transverse direction. The results are shown in a portion of the computational domain that is centered in the transverse direction and which is 13 μm wide.

A. Self-Supporting Pulses

Figure 1 shows the results of dispersion on a pulsed plane wave at four instants of time in its propagation. The pulse is started at the left-hand side of the domain. The dispersion in the material is characterized by a single Lorentzian resonance and is described by the following first-order susceptibility function: $\chi^{(1)}(\omega) = [\omega_0^2(\epsilon_s - \epsilon_\infty)]/(\omega_0^2 - \omega^2)$. Here $\epsilon_\infty = 9$, $\epsilon_s = 21$, and $\omega_0 = 6.0 \times 10^{14}$ rad/s. This dispersion is fictitious but is used to produce strong anomalous dispersion in a very

short distance (approximately $50 \mu\text{m}$). The wavelength of the plane wave is $\lambda = 1.55 \mu\text{m}$ (in vacuum), with the carrier frequency, ν_c , equal to 1.94×10^{14} Hz or $\omega_c = 1.22 \times 10^{15}$ rad/s, which is in the anomalous-dispersion range. The pulse has a hyperbolic secant envelope with a characteristic time constant of $T_0 = 10.3$ fs and a characteristic delay time constant of $T_D = 61.8$ fs. Notice that, as the wave propagates, the pulse lengthens owing to dispersion. Each oscillation in the pulse represents one wavelength.

Figure 2 shows the results of diffraction on a finite beam. Again the source is started at the left-hand side, and the four plots show the progression of the beam, including the beam's front edge. The cross-sectional profile of the beam source is a hyperbolic secant envelope with a characteristic width of $X_0 = 0.517 \mu\text{m}$, which is one wavelength of the optical carrier in a dielectric with an index of refraction equal to three. As the beam propagates, it widens owing to diffraction.

Figure 3 shows the effects of both dispersion and diffraction acting on a pulse. The parameters of dispersion and diffraction are those from the previous two calculations. Notice that the spreading rates of the pulse owing to dispersion and diffraction are approximately equal.

Figure 4 shows the pulse propagating under the combined effects of anomalous dispersion, diffraction, and nonlinear refraction. The length of the computational

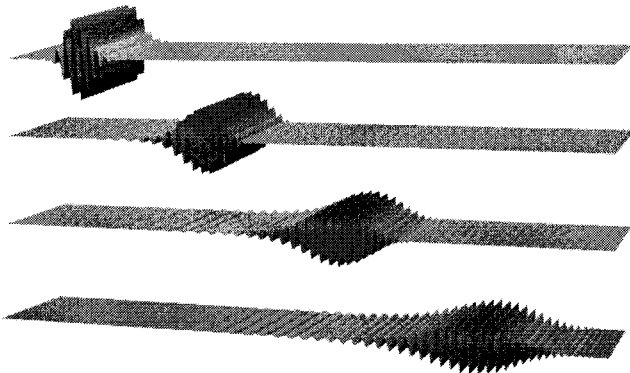


Fig. 1. Electric field of a plane wave in a dispersive medium after 155 fs, 310 fs, 465 fs, and 620 fs of propagation.

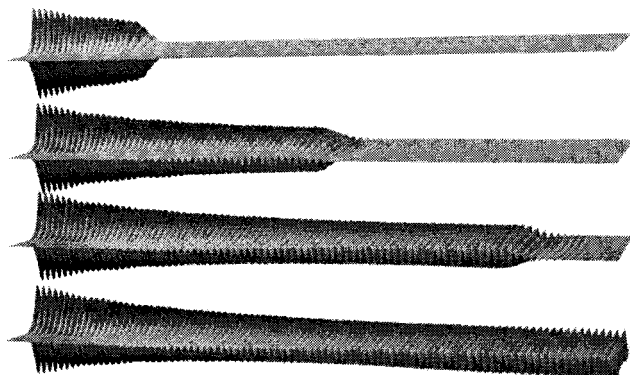


Fig. 2. Electric field of a beam undergoing diffraction after 155 fs, 310 fs, 465 fs, and 620 fs of propagation.

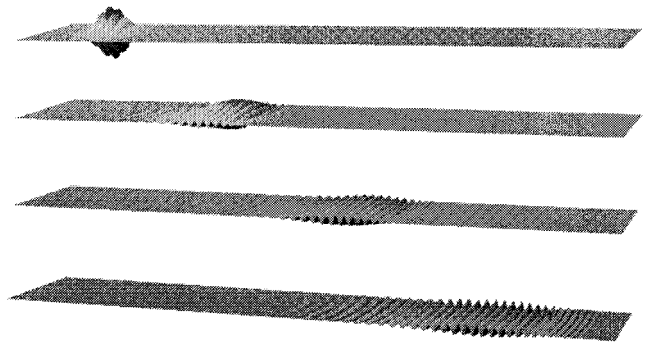


Fig. 3. Electric field of a pulse undergoing dispersion and diffraction after 155 fs, 310 fs, 465 fs, and 620 fs of propagation.

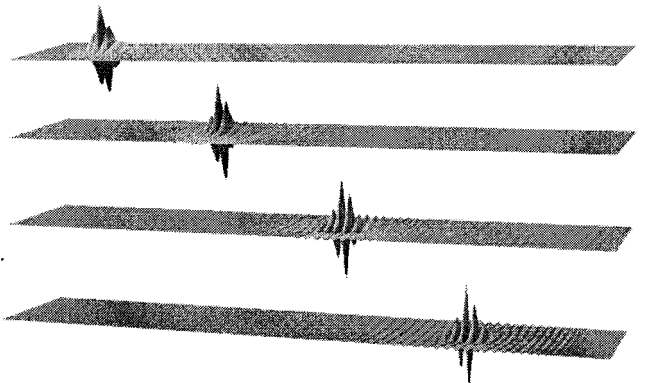


Fig. 4. Electric field of a pulse undergoing dispersion, diffraction, and nonlinear refraction after 155 fs, 310 fs, 465 fs, and 620 fs of propagation. Initial electric-field amplitude, $E_0 = 2.9 \times 10^{10}$ V/m; initial pulse width, $0.9 \mu\text{m}$ (FWHM); initial pulse duration, 18 fs (FWHM); pulse propagation distance, 28 Rayleigh ranges.

domain is reduced to $47 \mu\text{m}$ from $62 \mu\text{m}$. The strength of the nonlinearity, as given by the nonlinear index coefficient n_2^I , equals 3.2×10^{-20} m²/W (characteristic of silica at $\lambda = 1.55 \mu\text{m}$). The electric-field amplitude $E_0 = 2.9 \times 10^{10}$ V/m, which is extremely high. We found this value by varying the amplitude until the strength of the nonlinear effect of self-focusing could match the strengths of the linear effects of dispersion and diffraction. Notice that the pulse is now self-supporting, without any essential changes in size or shape. The wavelengths are distinguishable, and there are approximately five wavelengths in the pulse. Around the core of the pulse, which supports itself, is a surrounding low-intensity field of third-harmonic content, which disperses and diffracts away from the core. Also, as the pulse enters the domain, it compresses slightly from its initial shape and then retains that modified shape as it propagates further. So the initial shape, as determined by Eq. (10), is not the shape of the self-supporting pulse; rather, the pulse adjusts itself to that shape as it propagates. A video movie of the entire propagation showed that the pulse propagated smoothly with no instabilities. Also, it showed the progression of the optical carrier through the pulse envelope, since the phase velocity of the optical carrier was greater than the group velocity of the pulse. The pulse

propagated $\sim 36 \mu\text{m}$. The Rayleigh range z_0 is given by $\pi X_0^2/\lambda/n$ and is approximately $1.27 \mu\text{m}$. So the pulse travels essentially unchanged in shape over 28 times the Rayleigh range, which is a relatively long distance over which to test its self-support. In Subsection 3.C there are some examples of self-supporting pulse propagation over a distance of ~ 100 times the Rayleigh range.

It is interesting to compare the field value necessary to form this self-supporting pulse with the critical power for self-trapping^{25,39} in a bulk medium, i.e., $P_{\text{crit}} = [\pi(0.61)^2\lambda^2]/(8nn_2^I)$. Unlike in self-trapping, where the nonlinearity balances diffraction in two spatial directions, in our case the nonlinearity balances diffraction and dispersion. However, since the pulse parameters were chosen so that diffraction and dispersion occur at the same rate, we can expect that the same field strength will be needed to compensate for those. Indeed, we find that the field strength that will give a self-trapped beam with the same size is $E_0 = 2.93 \times 10^{10}$ V/m, as compared with $E_0 = 2.90 \times 10^{10}$ V/m in our pulse calculation. This close comparison starts diverging for calculations in the next subsection, where the variation of the GVD over the spectral range of the pulse becomes greater. Then the electric-field amplitude that is needed for self-support becomes larger than the value for self-trapping of a beam. But this breakdown in the comparison can be understood, since the comparison assumes that variations in the GVD are negligible.

Figure 5 shows a plot of the electric-field values along the centerline of the computational domain at the four times shown in the previous figure. Again this figure shows that the essential shape of the pulse is maintained. Figure 6 shows the temporal power spectrum of the pulse in the region of the carrier frequency at four locations along the centerline. Notice that the spectrum remains essentially unchanged. The complete power spectrum showed a small third-harmonic component.

Hence the results in Figs. 4–6 show that the pulse is essentially self-supporting, behaving similar to a light bullet. Also, calculations were performed in which the pulse traveled twice the distance shown in Fig. 4, and the pulse still maintained its support.

Figure 7 shows two counterpropagating pulses. Here the two pulses are identical to the pulse in the previous case, except that one pulse is entered into the domain

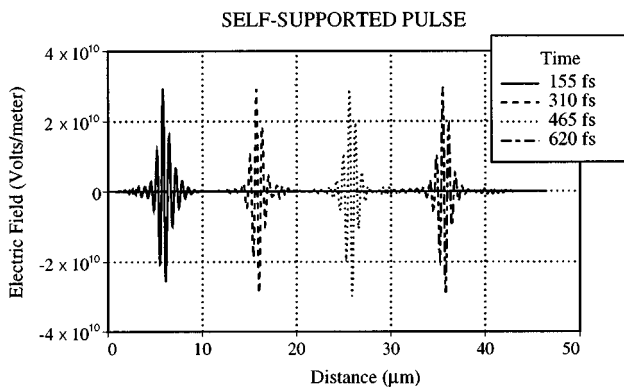


Fig. 5. Electric field along the centerline of the computational domain after 155 fs, 310 fs, 465 fs, and 620 fs of propagation. Initial pulse parameters are given in Fig. 4.

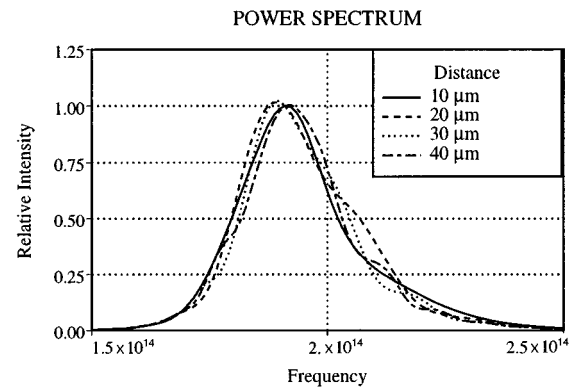


Fig. 6. Power spectrum of the pulse along the domain centerline and located at $10 \mu\text{m}$, $20 \mu\text{m}$, $30 \mu\text{m}$, and $40 \mu\text{m}$. Initial pulse parameters are given in Fig. 4.

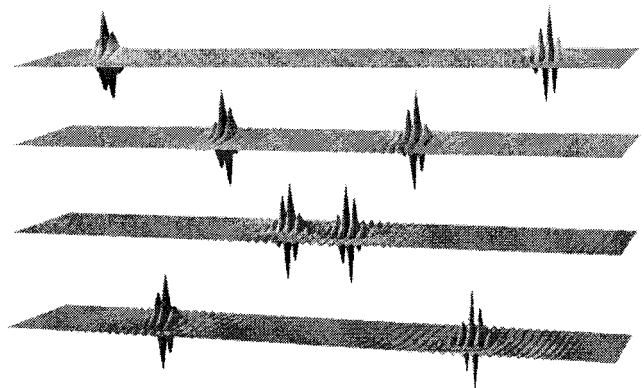


Fig. 7. Electric field of two counterpropagating pulses after 155 fs, 310 fs, 465 fs, and 620 fs of propagation. Initial pulse parameters are given in Fig. 4.

from the right-hand side. As in the previous case, both pulses propagated in self-supporting manners, as a video movie of the entire calculation showed. Also, the video showed the rapid constructive and destructive interference of the optical carriers of the two pulses as they passed through each other. A simulation of such effects is impossible with the NLSE, since the optical carrier is dropped from the description of the pulse. Comparisons of the rightward-moving pulse in Figs. 4 and 7 show that at 620 fs of travel the two pulses are almost identical, except for a very slight retardation in the interacting case as compared with the single-pulse case. Hence these pulses display the characteristics of solitons in being unchanged after undergoing collisions. After the collision, each pulse's trajectory is slightly changed through mutual attraction owing to nonlinear effects. Initially, the right-hand pulse is located slightly upward (a half-width, i.e., $0.26 \mu\text{m}$), in comparison with the left-hand pulse. At the third instant plotted, the pulses have just passed each other and the initially higher pulse is still slightly higher. By the fourth instant the two pulses become aligned vertically. Although the effect is small, and not observable in Fig. 7, more detailed plots show the altered paths. Hence these calculations show that one of these pulses can alter the path of another through an interaction. Such an interaction might form the basis of an optical switch. This calculation required only a minor modifica-

tion in the time-dependent boundary conditions from the case of one pulse, and the computer time required for the calculation remained the same. To do a similar calculation with the NLSE may require much larger modifications.

B. Pulse-Energy Variations

Additional calculations were made in which the energy of the pulse was varied about that at which the self-supporting pulse was found. The purpose of these additional calculations was to compare the results with the predictions of the NLSE. We made these additional calculations by varying the maximum electrical-field strength $E_0 \approx 2.9 \times 10^{10}$ V/m, which was the value that gave the results shown in Figs. 4–7. However, all the other parameters of the pulse and material were unchanged, such as the size and shape of the pulse and the dispersion parameters of the material. Calculations were performed in which the energy of the pulse (which is proportional to the square of the electrical-field strength) was 20% and 5% less, and 5%, 20%, and 90% greater, than that used previously. We analyzed the results by examining data that were displayed in plots like Figs. 4 and 5.

At 20% and 5% less energy, the pulses spread out because the energy was not sufficient for the size of the pulse, although at 5% less energy the pulse spread out very slowly. At 5% greater energy the pulse contracted more than the case shown in Figs. 4 and 5, but a self-supporting pulse was still formed, as shown in Fig. 8. At 20% greater energy the pulse initially self-focuses even more than previously, but then it spreads out rapidly, as shown in Fig. 9. In this case it appears that the self-focusing increases the dispersive and diffractive effects dynamically so that they overcome the self-focusing effects and ultimately spread the pulse out. At 90% greater energy the pulse initially self-focuses even more, but then it breaks up into two smaller pulses that spread out as in the previous case. This feature of the pulse, viz., initially compressing and then spreading out at higher energies, is similar to the results reported by Christov *et al.*¹⁵ In that simulation the slowly varying

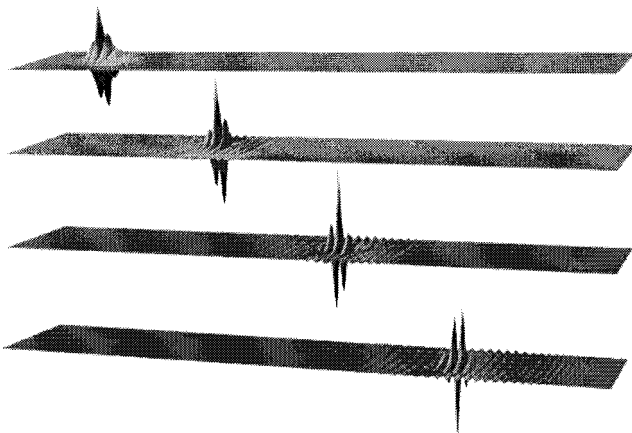


Fig. 8. Electric field of a pulse with 5% more energy after 155 fs, 310 fs, 465 fs, and 620 fs of propagation. Initial pulse parameters are the same as those given in Fig. 4, except here the initial electric-field amplitude is 5% greater.

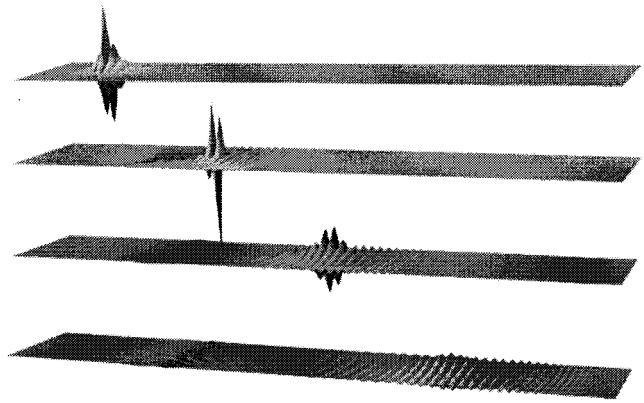


Fig. 9. Electric field of a pulse with 20% more energy after 155 fs, 310 fs, 465 fs, and 620 fs of propagation. Initial pulse parameters are the same as those given in Fig. 4, except here the initial electric-field amplitude is 20% greater.

envelope approximation was abandoned, and the peak power of the pulse was approximately 2 times the critical power.

By comparison the NLSE predicts² that above or below a critical energy the pulse will spread out or collapse, respectively. Here, in dramatic contrast, the pulse does not collapse above the small range in which self-support occurs, but in regions just above and below that range the pulse ultimately spreads out.

C. Light Bullets

Additional calculations were made to determine whether the energy range of the self-supporting pulses could be increased. The pulse duration and width were shortened, and the resonant frequency of the material was slightly increased. These changes were made so that we could increase the variation of the GVD acting on a pulse while still maintaining the approximate balance between the rates of dispersion and diffraction that were acting on the pulse. (The NLSE neglects the variation in the GVD, although higher-order dispersion can be modeled by adding terms to the NLSE.^{8,9}) For these calculations, $T_0 = 5.15$ fs and $X_0 = 0.259$ μm , i.e., these parameters were shortened to one-half of the values used previously and $\omega_0 = 6.1 \times 10^{14}$ rad/s, a slight increase from before.

By increasing the electric-field amplitude E_0 , we found a range of values within which the pulse was again self-supporting. Over that range, seven calculations were made for which E_0 was increased in equal increments from $E_0 = 6.17 \times 10^{10}$ V/m to $E_0 = 7.07 \times 10^{10}$ V/m. For $E_0 = 6.17 \times 10^{10}$ V/m the pulse spread out. For $E_0 = 7.07 \times 10^{10}$ V/m the pulse compressed slightly and then spread out in a manner similar to the case shown in Fig. 9. For the five cases in which E_0 varies from 6.30×10^{10} to 6.90×10^{10} V/m the pulse propagated in a self-supporting manner, similar to the cases shown in Figs. 4 and 8. Because of the reduction in the pulse size, the size of the computational domain was reduced. Now, the computational domain is 41 μm along the direction of propagation and 11 μm in the transverse direction. The results are shown in a portion of the computational domain that is centered in the transverse direction and which is 8 μm wide. Figures 10 and 11 show plots of the

electric-field values for E_0 equals 6.30×10^{10} and 6.90×10^{10} V/m, respectively. And Figs. 12 and 13 show the corresponding plots along the centerline of the computational domain. For both values of E_0 the plots show that initially the pulse amplitude decreases and then the pulse propagates in a self-supporting manner. The other three cases of intermediate energies showed similar self-supporting behavior. Here the energy variation for which the pulses are self-supporting is $\sim 20\%$. These pulses traveled $\sim 30 \mu\text{m}$, and, because of their narrower widths compared with the previous cases, this distance is ~ 100 times their Rayleigh range. The more-energetic

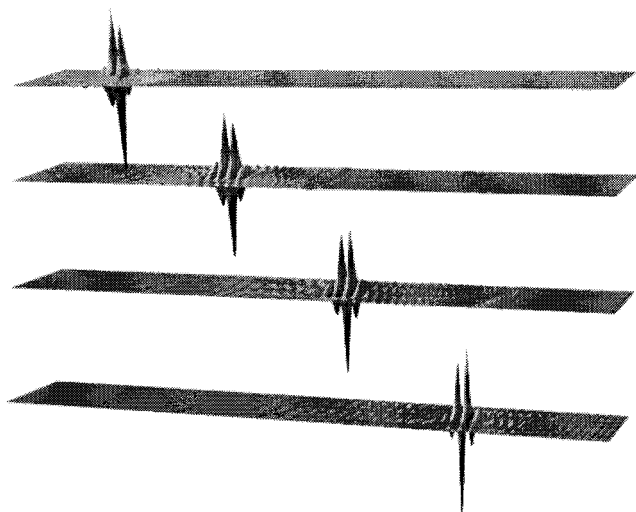


Fig. 10. Light bullet: Electric field after 136 fs, 272 fs, 408 fs, and 544 fs of propagation. Initial electric-field amplitude, $E_0 = 6.3 \times 10^{10}$ V/m; initial pulse width, $0.45 \mu\text{m}$ (FWHM); initial pulse duration, 9 fs (FWHM); pulse propagation distance, 100 Rayleigh ranges.

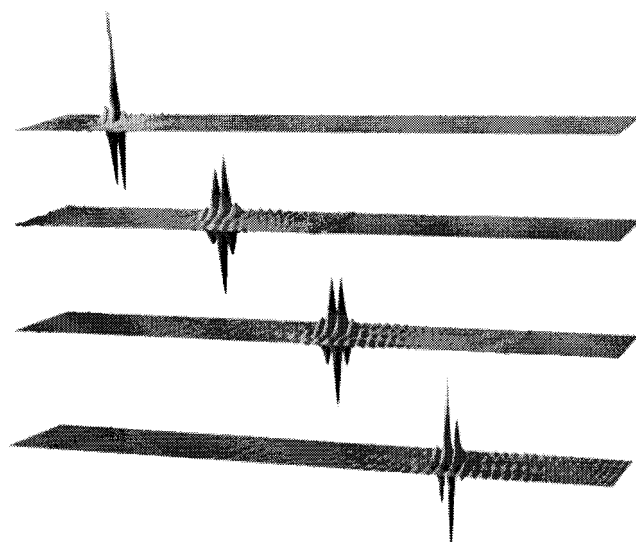


Fig. 11. Light bullet: Electric field after 136 fs, 272 fs, 408 fs, and 544 fs of propagation. Initial pulse parameters are the same as those given in Fig. 10, except here the pulse energy is greater with the larger initial electric-field amplitude $E_0 = 6.9 \times 10^{10}$ V/m.

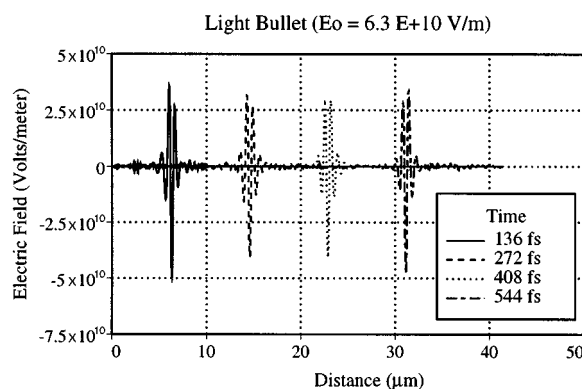


Fig. 12. Light bullet: Electric field along the centerline of the computational domain after 136 fs, 272 fs, 408 fs, and 544 fs of propagation. Pulse parameters are given in Fig. 10.

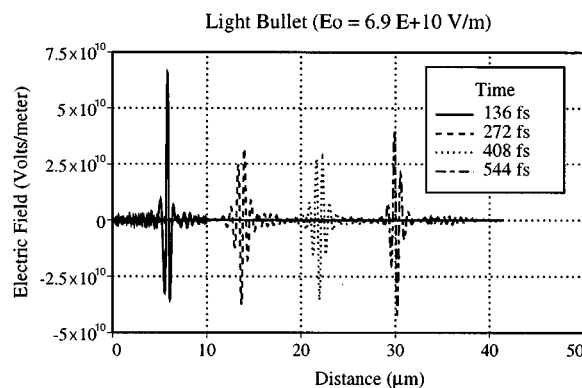


Fig. 13. Light bullet: Electric field along the centerline of the computational domain after 136 fs, 272 fs, 408 fs, and 544 fs of propagation. Pulse parameters are given in Fig. 11.

pulse, as shown in Fig. 13, traveled slightly less than the less-energetic pulse, as shown in Fig. 12, because of the increased nonlinear refraction acting on it. With these distances of self-support over a 20% energy variation these pulses act like light bullets.

These calculations show that the variation in the GVD provides a means for stabilizing the pulse, as long as the energy of the pulse does not get too large. This effect of the GVD on a pulse is analogous²⁵ to the stabilizing effect of the saturation of the nonlinear index on the self-focusing of a beam.

4. CONCLUSIONS

Light bullets have been found in numerical simulations of optical pulse propagation in planar waveguides when the complete Maxwell equations are used without making the slowly varying envelope approximation. The energy range for which these pulses are stable depends on the pulse and material parameters, and above that range the pulses do not collapse but rather expand after initially compressing. In contrast, the standard NLSE predicts² that self-focusing will lead to the collapse of optical pulses when a certain critical power is exceeded. The predictions of the NLSE break down when the variation in the GVD dispersion becomes significant. Here that variation has been found to stabilize the self-supporting pulses so

that they can be regarded as light bullets. These initial calculations looked at just a few choices of parameter values for the pulse and the material that determined the effects of dispersion, diffraction, and nonlinear refraction. There may be other values for which the pulses could be stable over a larger energy range and for which the energy requirements are more modest.

Also, it was found that two of these counterpropagating pulses changed each other's direction by nonlinear attraction while colliding. The algorithm used for these simulations is fairly general and has the capability of including linear and nonlinear dispersive and absorptive effects, as well as instantaneous nonlinear effects. The dynamics of the optical carrier are resolved in this method. The calculations were performed on a Cray C-90 computer and took from 100 to 500 s per case, depending of the length of the propagation, so these calculations were relatively minor ones.

REFERENCES

- P. M. Goorjian and Y. Silberberg, "Numerical simulations of light bullets, using the full vector, time dependent, nonlinear Maxwell equations," in *Integrated Photonics Research*, Vol. 7 of 1995 OSA Technical Digest Series (Optical Society of America, Washington, D.C., 1995), pp. 84–86.
- Y. Silberberg, "Collapse of optical pulses," *Opt. Lett.* **15**, 1282–1284 (1990).
- P. M. Goorjian and A. Taflove, "Direct time integration of Maxwell's equations in nonlinear dispersive media for propagation and scattering of femtosecond electromagnetic solitons," *Opt. Lett.* **17**, 180–182 (1992).
- P. M. Goorjian, A. Taflove, R. M. Joseph, and S. C. Hagness, "Computational modeling of femtosecond optical solitons from Maxwell's equations," *IEEE J. Quantum Electron.* **28**, 2416–2422 (1992).
- P. M. Goorjian, A. Taflove, and R. M. Joseph, "Calculations of femtosecond optical solitons from the vector nonlinear Maxwell's equations," in *Short Wavelength V: Physics with Intense Laser Pulses*, M. D. Perry and P. B. Corkum, eds., Vol. 17 of OSA Proceedings Series (Optical Society of America, Washington, D.C., 1993), pp. 66–69.
- P. M. Goorjian, A. Taflove, and R. M. Joseph, "Calculations of femtosecond temporal solitons and spatial solitons using the vector Maxwell's equations," in *Nonlinear Guided-Wave Phenomena*, Vol. 15 of 1993 OSA Technical Digest Series (Optical Society of America, Washington, D.C., 1993), pp. 228–231.
- B. E. A. Saleh and M. C. Teich, *Fundamentals of Photonics* (Wiley, New York, 1991).
- G. P. Agrawal, *Nonlinear Fiber Optics*, 2nd ed. (Academic, New York, 1995).
- G. P. Agrawal and C. Headley, "Kink solitons and optical shocks in dispersive nonlinear media," *Phys. Rev. A* **46**, 1573–1577 (1992).
- R. L. Fork, C. H. Brito Cruz, P. C. Becker, and C. V. Shank, "Compression of optical pulses to six femtoseconds by using cubic phase compensation," *Opt. Lett.* **12**, 483–485 (1987).
- M. T. Asaki, C. P. Huang, D. Garvey, J. Zhou, H. C. Kapteyn, and M. M. Murnane, "Generation of 11-fs pulses from a self-mode-locked Ti:sapphire laser," *Opt. Lett.* **18**, 977–979 (1993).
- J. Zhou, G. Taft, C. P. Huang, M. M. Murnane, and H. C. Kapteyn, "Pulse evolution in a broad-bandwidth Ti:sapphire laser," *Opt. Lett.* **19**, 1149–1151 (1994).
- D. T. Walton, J. Nees, and G. Mourou, "Broad-bandwidth pulse amplification to the 10- μ J level in an ytterbium-doped germanosilicate fiber," *Opt. Lett.* **21**, 1061–1063 (1996).
- A. Baltuska, Z. Wei, M. S. Pshenichnikov, and D. A. Wiersma, "Optical pulse compression to 5 fs at a 1-MHz repetition rate," *Opt. Lett.* **22**, 102–104 (1997).
- I. P. Christov, H. C. Kapteyn, M. M. Murnane, C. P. Huang, and J. Zhou, "Space-time focusing of femtosecond pulses in a Ti:sapphire laser," *Opt. Lett.* **20**, 309–311 (1995).
- I. P. Christov, V. D. Stoev, M. M. Murnane, and H. C. Kapteyn, "Mode locking with a compensated space-time astigmatism," *Opt. Lett.* **20**, 2111–2113 (1995).
- I. P. Christov, V. D. Stoev, M. M. Murnane, and H. C. Kapteyn, "Sub-10-fs operation of Kerr-lens mode-locked lasers," *Opt. Lett.* **21**, 1493–1495 (1996).
- D. Huang, M. Ulman, L. H. Acioli, H. A. Haus, and J. G. Fujimoto, "Self-focusing-induced saturable loss for laser mode locking," *Opt. Lett.* **17**, 511–513 (1992).
- G. G. Luther, J. V. Moloney, A. C. Newell, and E. M. Wright, "Self-focusing threshold in normally dispersive media," *Opt. Lett.* **19**, 862–864 (1994).
- G. G. Luther, A. C. Newell, and J. V. Moloney, "The effects of normal dispersion on collapse events," *Physica D* **74**, 59–73 (1994).
- A. S. Kewitsch and A. Yariv, "Self-focusing and self-trapping of optical beams upon photopolymerization," *Opt. Lett.* **21**, 24–26 (1996).
- X. Liu and D. Umstadter, "Self-focusing of intense subpicosecond laser pulses in a low pressure gas," in *Short Wavelength V: Physics with Intense Laser Pulses*, M. D. Perry and P. B. Corkum, eds., Vol. 17 of OSA Proceedings Series (Optical Society of America, Washington, D.C., 1993), pp. 45–49.
- A. Braum, G. Korn, X. Liu, D. Du, J. Squier, and G. Mourou, "Self-channeling of high-peak-power femtosecond laser pulses in air," *Opt. Lett.* **20**, 73–75 (1995).
- A. Brodeur, C. Y. Chien, F. A. Ilkov, S. L. Chin, O. G. Kosareva, and V. P. Kandidov, "Moving focus in the propagation of ultrashort laser pulses in air," *Opt. Lett.* **22**, 304–306 (1997).
- Y. R. Shen, *The Principles of Nonlinear Optics* (Wiley, New York, 1984), Chap. 17.
- G. D. Sucha, "Continuum generation in the infrared using a femtosecond color-center laser system," Ph.D. dissertation (University of Rochester, Rochester, New York, 1991).
- Y. Chen and J. Atai, "Dark optical bullets in light self-trapping," *Opt. Lett.* **20**, 133–135 (1995).
- A. W. Snyder and J. D. Mitchell, "Mighty morphing spatial solitons and bullets," *Opt. Lett.* **22**, 16–18 (1997).
- J. E. Rothenburg, "Pulse splitting during self-focusing in normally dispersive media," *Opt. Lett.* **17**, 583–585 (1992).
- J. E. Rothenburg, "Space-time focusing: breakdown of the slowly varying envelope approximation in the self-focusing of femtosecond pulses," *Opt. Lett.* **17**, 1340–1342 (1992).
- N. Akhmediev and A. Ankiewicz, "Does the nonlinear Schrödinger equation correctly describe beam propagation?" *Opt. Lett.* **18**, 411–413 (1993).
- A. W. Snyder, J. D. Mitchell, and Y. Chen, "Spatial solitons of Maxwell's equations," *Opt. Lett.* **19**, 524–526 (1994).
- K. Hayata and M. Koshiba, "Multidimensional solitons in cubic nonlinear media," *Opt. Lett.* **19**, 1717–1719 (1994).
- N. F. Borrelli, B. G. Aitken, and M. A. Newhouse, "Resonant and non-resonant effects in photonic glasses," *J. Non-Cryst. Solids* **185**, 109–122 (1995).
- R. G. Flesch, A. Pushkarev, and J. V. Moloney, "Carrier wave shocking of femtosecond optical pulses," *Phys. Rev. Lett.* **76**, 2488–2499 (1996).
- W. Forysiak, R. G. Flesch, J. V. Moloney, and E. M. Wright, "Doppler shift of self-reflected optical pulses at an interface: dynamic nonlinear optical skin effect," *Phys. Rev. Lett.* **76**, 3695–3698 (1996).
- P. M. Goorjian and G. P. Agrawal, "Computational modeling of ultrafast optical pulse propagation in nonlinear optical materials," in *Nonlinear Optics: Materials, Fundamentals, and Applications*, Vol. 11 of 1996 OSA Technical Digest Series (Optical Society of America, Washington, D.C., 1996), pp. 132–133.
- J. D. Jackson, *Classical Electrodynamics*, 2nd ed. (Wiley, New York, 1975).
- R. W. Boyd, *Nonlinear Optics* (Academic, New York, 1992).